Resistive transition in frustrated Josephson-junction arrays on a honeycomb lattice

Enzo Granato

Laboratório Associado de Sensores e Materiais, Instituto Nacional de Pesquisas Espaciais, 12227-010 São José dos Campos, SP Brazil

(Received 20 November 2012; revised manuscript received 14 February 2013; published 21 March 2013)

We use driven Monte Carlo dynamics to study the resistive behavior of superconducting Josephson-junction arrays on a honeycomb lattice in a magnetic field corresponding to f flux quantum per plaquette. While for $f = 1/3$ the onset of zero resistance is found at nonzero temperature; for $f = 1/2$ the results are consistent with a transition scenario where the critical temperature vanishes and the linear resistivity shows thermally activated behavior. We determine the thermal critical exponent of the zero-temperature transition for $f = 1/2$ from a dynamic scaling analysis of the nonlinear resistivity. The resistive behavior agrees with recent results obtained for the phase-coherence transition from correlation-length calculations and with experimental observations on ultrathin superconducting films with a triangular pattern of nanoholes.

DOI: 10.1103/PhysRevB.87.094517 PACS number(s): 74.81.Fa, 74.25.Uv, 75.10.Nr

I. INTRODUCTION

Josephson-junction (JJ) arrays have remarkable properties in a magnetic field that are strongly dependent on the geometry of the structure. In addition to being realized as two-dimensional arrays of weakly coupled superconducting grains,[1–3] they provide important models for superconducting wire networks[4–7] and other inhomogeneous superconducting systems, when phase fluctuations of the superconducting order parameter play a major role.[8] An idealized JJ array is equivalent to the frustrated XY model,[9] where frustration can be tuned by the applied external magnetic field. The frustration parameter f, corresponding to the number of flux quantum per plaquette of the array, sets the average density of vortices in the lattice of pinning sites formed by the plaquette centers. Depending on the topology of the lattice of pinning sites and the value of f, a commensurate vortex lattice is favored in the ground state, allowing for a phase-coherence transition at finite temperature. In this case, the equilibrium phase transitions and resistive behavior of the superconducting array are reasonably well understood for simple, low-order commensurate phases such as $f = 1/2$ on a square array[9] and $f = 1/3$ on a honeycomb array.[10] The magnetoresistance for a square JJ array, for example, oscillates with the applied magnetic field,[1,2,6] displaying minima at integer values of f and secondary minima at $f = 1/2$ for decreasing temperatures, corresponding to resistive transitions at different temperatures.[9] The onset of zero resistance for decreasing temperatures marks the phase-coherence transition in the JJ array, which for integer f is expected to be in the Koterlitz-Thouless (KT) universality class. Dynamical transitions under an external driving current have also been studied for $f = 1/2$ on a square lattice, leading to interesting nonequilibrium phase diagrams.[11] However, when the vortex lattice is incommensurate with the pinning sites, as for irrational f on a square JJ array[3,5,6,12–16] or $f = 1/2$ on a honeycomb JJ array,[7,10,17–19] the possible phase transitions are much less understood, showing some features of a vortex glass without disorder and dynamical freezing at low temperatures. In particular, a JJ array on a honeycomb lattice with $f = 1/2$ should display interesting resistive behavior. As a model of phase fluctuations, it should be relevant to ultrathin superconducting films with a periodic pattern of nanoholes,[20,21] which can be regarded as a lattice of pinning centers. While for a square lattice of nanoholes, the magnetoresistance oscillates with the applied field, displaying secondary minima at $f = 1/2$ as for a square JJ array,[20] for a triangular lattice[21] it shows only minima at integer flux quantum per lattice unit cell.

In early Monte Carlo (MC) simulations of the fully frustrated XY model on a honeycomb lattice,[10] a phase-coherence transition at a nonzero temperature in the KT universality class was suggested and therefore a resistive transition would be expected for a JJ array in the same lattice with $f = 1/2$. On the other hand, a different calculation[17] suggested a spin-glass-like transition. It was also suggested[22] that only a crossover region rather than an equilibrium phase transition should occur at any nonzero temperature. Recently,[18] it was argued that vortex-ordered phases could be possible at nonzero temperatures but for very large systems, beyond the ones currently studied numerically or even experimentally. However, the question of the resistive transition was not investigated. In a recent MC study of phase coherence in the fully frustrated XY model, a zero-temperature transition scenario[19] was proposed, where $T_c = 0$ but the divergent correlation length, $\xi \propto T^{-\nu}$, should lead to measurable effects at finite temperatures in the linear and nonlinear resistivity, determined by the thermal critical exponent ν. So far, a direct calculation of the resistive behavior of JJ arrays on a honeycomb lattice and comparison to experiments have not been presented.

In this work, we present results for the resistive behavior obtained by driven Monte Carlo dynamics. While for $f = 1/3$ a resistive transition is found at nonzero temperature, for $f = 1/2$ the results are consistent with a transition scenario where the critical temperature vanishes and the linear resistivity shows thermally activated behavior. We determine the thermal critical exponent ν of the zero-temperature transition for $f = 1/2$ from a dynamic scaling analysis of the nonlinear resistivity. Its value is in fair agreement with recent calculations for the frustrated XY model from finite-size correlation length scaling.[19] A dynamical freezing at lower temperatures is also identified from deviations of the fluctuation-dissipation relation between linear resistivity and voltage autocorrelations. The resistive behavior is consistent with some experimental observations in ultrathin superconducting films with a triangular lattice of nanoholes,[21] taking into account the effects of weak Josephson-coupling disorder.

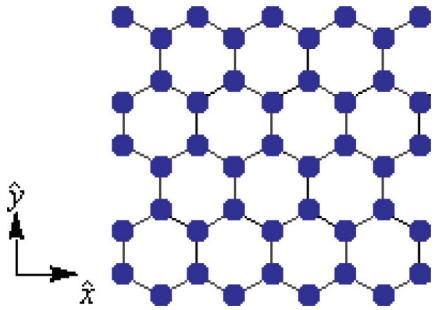

FIG. 1. (Color online) JJ array on a honeycomb lattice. Filled circles represent superconducting grains and the lines the Josephson junctions between them.

II. MODEL AND DRIVEN MONTE CARLO SIMULATION

We consider a JJ array in a uniform transverse magnetic field described by the Hamiltonian

$$H = -\sum_{\langle ij \rangle} J_{ij} \cos(\theta_i - \theta_j - A_{ij}) - J \sum_i (\theta_i - \theta_{i+\hat{x}}), \quad (1)$$

where θ_i is the phase of the local superconducting order parameter of the grains located on the sites of a two-dimensional honeycomb lattice with lattice spacing a, as illustrated in Fig. 1. The first term is the contribution from the Josephson-coupling energy between nearest-neighbor grains. For uniform coupling we set $J_{ij} = J_o$, a constant independent of the magnetic field. The line integral of the vector potential A_{ij} due to the external field $\vec{B} = \nabla \times \vec{A}$ is constrained to $\sum_{ij} A_{ij} = 2\pi f$ around each hexagonal plaquette, where f is the number of flux quantum $\phi_o = hc/2e$ per plaquette. This model is periodic in f with period $f = 1$. In the calculations we choose a gauge where $A_{ij} = 2\pi f n_i/2$ on the (tilted) bonds along the horizontal rows numbered by the integer n_i and $A_{ij} = 0$ on the vertical bonds of the lattice. The second term in Eq. (1) represents the effects of an external driving current density $(2e/\hbar)J$ applied in the $\hat{x}$ (horizontal) direction, coupling to the phase difference, $\theta_i - \theta_{i+\hat{x}}$, between nearest-neighbor sites in this direction. When $J \neq 0$, the total energy is unbounded and the system is out of equilibrium. The lower-energy minima occur at phase differences $\theta_i - \theta_{i+\hat{x}}$, which increases with time t, leading to a net phase slippage rate proportional to $< d(\theta_i - \theta_{i+\hat{x}})/dt >$, corresponding to the voltage $V_{i,i+\hat{x}}$. For convenience, we use units where $2e/\hbar = 1$, $J_o = 1$, and $a = 1$.

To study the current-voltage behavior, we use a driven MC dynamics method.[23] The time dependence is obtained by identifying the MC time as the real time t and we set the unit of time $dt = 1$, corresponding to a complete MC pass through the lattice. For convenience, the honeycomb lattice is defined on a rectangular geometry (Fig. 1), with linear size given by a dimensionless length L. In terms of L, the linear size in the $\hat{x}$ and $\hat{y}$ directions can be written as $L_x = L\sqrt{3}a$ and $L_y = \frac{3}{2}a$, respectively. This corresponds to $2L$ junctions along the horizontal rows. The usual periodic boundary conditions are used in the $\hat{y}$ direction and periodic (fluctuating twist) boundary conditions[24] in the $\hat{x}$ direction. The twist boundary condition adds new dynamical variables u_x, corresponding to a uniform phase twist between nearest-neighbor sites along the $\hat{x}$ direction. An MC step consists of an attempt to change the local phases θ_i and the phase twist u_x using the Metropolis algorithm. If the change in energy is ΔH, the trial move is accepted with probability $\min\{1, \exp(-\Delta H/kT)\}$. The external current density J in Eq. (1) biases these changes, leading to a net voltage (phase slippage rate) across the system in the $\hat{x}$ direction given by

$$V = 2L \frac{d}{dt} u_x, \quad (2)$$

in arbitrary units. Compared to the usual Langevin dynamics,[15] this MC method allows access to much longer time scales, which is required to obtain reliable data at lower temperatures and current densities. We have determined the electric field $E = V/(2L)$ and nonlinear resistivity $\rho = E/J$ as a function of the driving current density J, in the $\hat{x}$ direction, for different temperatures T and different system sizes L. We used typically 5×10^6 MC steps to reach the nonequilibrium steady state and equal time steps to perform time averages, with additional averages over 6–12 independent runs. In an MC step, the maximum changes in the local phases θ_i and the phase twist u_x were fixed to $\pm\pi$ and $\pm\pi/(2L)$, respectively.

The linear resistivity, $\rho_L = \lim_{J->0} E/J$, can be determined from the nonlinear behavior $\rho(J)$ obtained from the driven MC simulations by extrapolating the numerical results to vanishing currents. It can also be obtained, independently, from equilibrium voltage fluctuations and therefore can be calculated in the absence of an imposing driving current ($J = 0$). From the Kubo formula, the linear resistance is given in terms of the equilibrium voltage autocorrelation as

$$R_L = \frac{1}{2T} \int dt \langle V(t)V(0) \rangle. \quad (3)$$

Since the total voltage V is related to the phase difference across the system $\Delta\theta(t)$ by $V = d\Delta\theta(t)/dt$, we find it more convenient to determine R_L from the long-time equilibrium fluctuations[25] of $\Delta\theta(t)$ as

$$R_L = \frac{1}{2Tt} \langle [\Delta\theta(t) - \Delta\theta(0)]^2 \rangle, \quad (4)$$

which is valid for sufficiently long times t.

III. RESULTS AND DISCUSSION

First, we consider the resistive behavior when $f = 1/3$. For this value of the frustration, it is known that a hexagonal vortex lattice commensurate with the honeycomb lattice is the ground state[10] and therefore a resistive transition would be expected at a temperature smaller than or equal to the vortex lattice melting. Figure 2 shows the nonlinear resistivity E/J as a function of temperature, for the largest system size $L = 60$, where finite-size effects are small. For decreasing current densities J, the nonlinear resistivity E/J tends to a finite value at high temperatures, corresponding to the linear resistivity ρ_L, but extrapolates to very low values at lower temperatures. This behavior is consistent with a resistive transition occurring at a critical temperature in the range $T_c(f = 1/3) = 0.224$–0.225. In fact, it is slightly smaller than the vortex lattice melting transition estimated from recent equilibrium MC simulations of the frustrated XY model on a honeycomb lattice,[19]

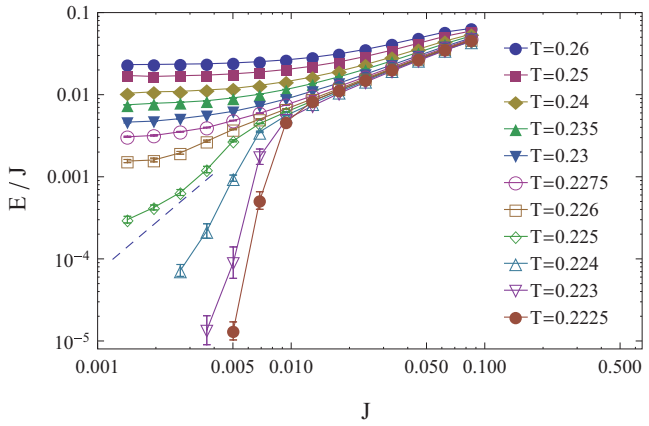

FIG. 2. (Color online) Nonlinear resistivity E/J as a function of current density J at different temperatures T for $f = 1/3$. System size $L = 60$. The dashed line indicates power-law behavior $E \propto J^3$.

$T_m = 0.226(1)$. At the resistive transition, a power-law relation $E \propto J^{z+1}$ is expected at sufficiently small currents from the scaling theory,[26] where z is the dynamical critical exponent. For the usual KT transition it is known[2,26] that $z = 2$. In the present case, as shown by the dashed line in Fig. 2, a power law separating the $T > T_c$ from $T < T_c$ behavior at small currents is compatible with $z = 2$. However, further work taking into account finite-size effects is required to investigate the critical behavior in detail. In any case, the above results show clear evidence of a resistive transition at finite temperature for $f = 1/3$.

In contrast to the resistive behavior in Fig. 2, when $f = 1/2$ the nonlinear resistivity E/J tends to a finite value for decreasing currents even at low temperatures, as shown in Fig. 3. Although we cannot exclude a transition at much lower temperatures, where reliable data could not be obtained as discussed below, this behavior is consistent with a resistive transition occurring only at zero temperature. Recent equilibrium MC simulations suggested such a zero-temperature transition scenario,[19] where $T_c = 0$ for the phase-coherence transition but the finite correlation length for $T > 0$ leads to measurable effects in the nonlinear resistivity. In fact,

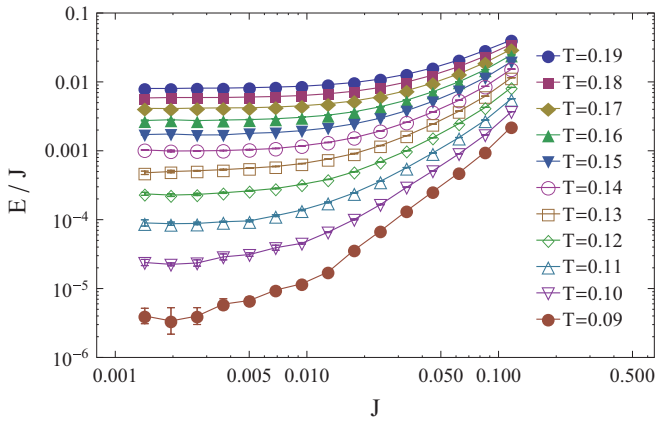

FIG. 3. (Color online) Nonlinear resistivity E/J as a function of current density J at different temperatures T for $f = 1/2$. System size $L = 60$.

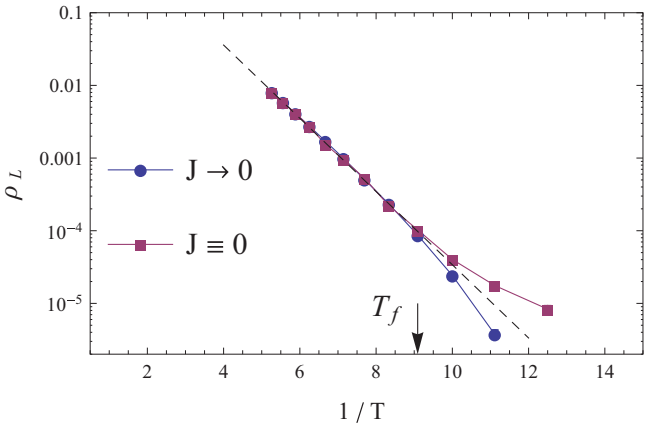

FIG. 4. (Color online) Temperature dependence of the linear resistivity ρ_L for $f = 1/2$ obtained from nonlinear resistivity ($J \to 0$) and from voltage fluctuations ($J \equiv 0$). System size $L = 60$. The separation of the curves gives an estimate of the dynamical freezing temperature T_f. The dashed line is an Arrhenius fit for $T > T_f$.

the behavior in Fig. 3 has the main features expected for a zero-temperature resistive transition. The linear resistivity ρ_L, corresponding to a zero current limit of E/J, decreases rapidly with decreasing temperature and for increasing J, E/J crosses over to a nonlinear behavior at a characteristic current density J_{nl}, which also decreases with decreasing temperature.

To verify in which temperature range the values approached at low currents in Fig. 3 correspond indeed to the linear resistivity ρ_L, we show in Fig. 4 the temperature dependence of ρ_L obtained from the nonlinear resistivity as $\rho_L = \lim_{J->0} E/J$ and, without current bias, from Eq. (3). These values obtained from nonequilibrium and equilibrium calculations agree with each other above a temperature $T_f \sim 0.11$ and deviate significantly at lower temperatures. Since this agreement is only expected when the voltage autocorrelation in Eq. (3) is obtained in true equilibrium, one can regard T_f as a signature of a dynamical freezing transition below which equilibrium is not achieved due to very large relaxation time. Interestingly, a dynamical freezing transition near the same temperature was also identified in recent equilibrium MC simulations by other methods and different dynamics.[19] The apparent KT transition[10] and spin-glass transition[17] observed in earlier MC simulations could be attributed to slow dynamics effects of such dynamical freezing.

The straight-line behavior of $\rho_L(T)$ for $T > T_f$ in the log-linear plot of Fig. 4 indicates an activated Arrhenius behavior, where the linear resistivity decreases exponentially with the inverse of temperature with a temperature-independent energy barrier, estimated as $E_b = 1.16(4)J_o$. If such behavior extrapolates to lower temperatures, it suggests that the linear resistivity can be very small but nevertheless remains finite for decreasing temperatures, and therefore there is no resistive transition at finite temperatures. However, as will be described below, the system behaves as if a resistive transition occurs at zero temperature, corresponding to a phase-coherence transition where the critical temperature vanishes, $T_c = 0$.

A detailed scaling theory[26] of the resistive transition with $T_c = 0$ has been described in the context of the current-voltage characteristics of vortex-glass models[25–27] of disordered

two-dimensional superconductors, but the arguments should also apply to the present case. The basic assumption is the existence of a second-order phase transition. The correlation length ξ is finite for $T > 0$ but it increases with decreasing temperature as $\xi \propto T^{-\nu}$, with ν a critical exponent. The divergent correlation length and relaxation time τ near the transition determine both the linear and nonlinear resistivity behavior leading to current-voltage scaling sufficiently close to the critical temperature and sufficiently small driving current. If the data satisfy such scaling behavior for different driving currents and temperatures, the critical temperature and critical exponents of the underlying equilibrium transition at $J = 0$ can then be determined from the best data collapse. The dimensionless ratio $E/J\rho_L$ should satisfy the scaling form[26]

$$\frac{E}{J\rho_L} = g\left(\frac{J}{T^{1+\nu}}\right), \tag{5}$$

where g is a scaling function with $g(0) = 1$. A crossover from linear behavior, when $g(x) \sim 1$, to nonlinear behavior, when $g(x) \gg 1$, occurs when $x \sim 1$, which leads to a crossover current density at which nonlinear behavior sets in, decreasing with temperature as a power law, $J_{nl} \propto T/\xi \propto T^{1+\nu}$. The scaling form in Eq. (5) contains a single critical exponent ν and does not depend on the particular form assumed for the divergence of the relaxation time τ. However, for sufficiently low temperatures, the relaxation process is expected to be thermally activated,[26] with $\tau \propto \exp(E_b/kT)$. This corresponds formally to a dynamic exponent $z \to \infty$, if power-law behavior is assumed for the relaxation time $\tau \propto \xi^z$. The linear resistivity should scale as[26] $\rho_L \propto 1/\tau$ and therefore it is also expected to have an activated behavior, $\rho_L \propto \exp(-E_b/kT)$. In general, the energy barrier E_b also scales with the correlation length as $E_b \propto \xi^{\psi}$, which leads to a temperature-dependent barrier $E_b \propto T^{-\psi\nu}$. A pure Arrhenius behavior corresponds to $\psi = 0$.

The behavior of the nonlinear and linear resistivity in Figs. 3 and 4 above the dynamical freezing temperature T_f are quite consistent with the predictions from the scaling theory. Figure 5 shows the temperature dependence of the crossover current J_{nl}, defined as the value of J where $E/J\rho_L$ starts to deviate from a fixed value, chosen to be $c = 1.2$. For the lowest temperature range above T_f, the linear behavior in the log-log plot is consistent with the expected power law $J_{nl} \propto T^{1+\nu}$ for a zero-temperature transition. From the power-law fit we obtain a first estimate of the exponent $\nu = 1.17(14)$. In contrast, for $f = 1/3$, the behavior in the lowest temperature range does not allow a similar power-law fit; J_{nl} curves down for decreasing temperatures and extrapolates to zero at a finite temperature, consistent with a resistive transition at a nonzero critical temperature found for $f = 1/3$. The nonlinear resistivity data also satisfies the scaling form for different driving currents and temperatures. Figure 6 shows a scaling plot of the nonlinear resistivity above T_f according to Eq. (5) for a large system size $L = 60$ where the finite-size dependence is small. The best data collapse provides an estimate of the critical exponent $\nu = 1.40(9)$. The data collapse is achieved quantitatively by means of a least-squares fit method,[19,28] varying the parameter ν. The scaling function $g(x)$ is approximated by a Taylor series expansion for small x, truncated beyond fourth order, which is used to fit the data and provide the least-squares residuals. The error estimate here corresponds to the statistical error from the least-squares method and does not include systematic effects. To check for systematic errors from finite-size effects, which were assumed negligible in the scaling form of Eq. (5), the same data collapse procedure was repeated for larger system sizes, as shown in Fig. 7. The results of these estimates, $\nu = 1.36(8)$ for $L = 72$ and $1.33(8)$ for $L = 90$, agree within the statistical errors but indicate that the central estimate of ν decreases slowly with system size. The nonlinear resistivity should also satisfy the expected finite-size behavior in smaller system sizes when the correlation length ξ approaches the system size L. According to finite-size scaling, the scaling function in Eq. (5) should also depend on the dimensionless ratio L/ξ and so, to account for finite-size effects, the nonlinear resistivity should satisfy the scaling form

$$\frac{E}{J\rho_L} = \bar{g}\left(\frac{J}{T^{1+\nu}}, L^{1/\nu}T\right). \tag{6}$$

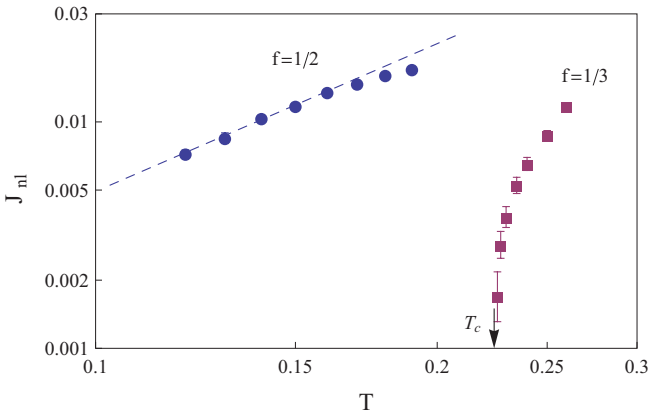

FIG. 5. (Color online) Temperature dependence of the crossover current J_{nl} for $f = 1/2$ and $f = 1/3$. System size $L = 60$. The dashed line is a power-law fit to $J_{nl} \propto T^{1+\nu}$, giving the estimate $\nu = 1.17(14)$. The arrow indicates the estimated critical temperature for $f = 1/3$.

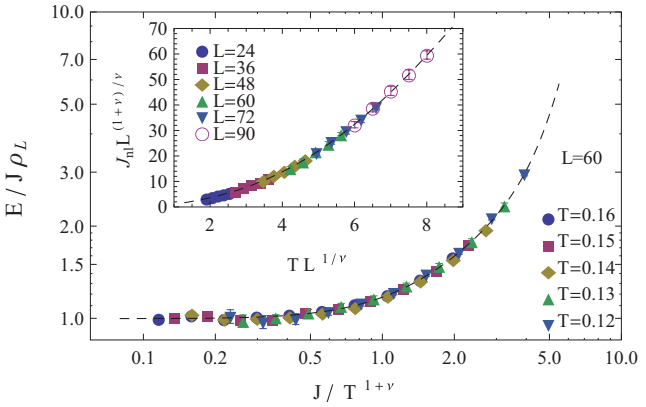

FIG. 6. (Color online) Scaling plot of the nonlinear resistivity E/J from Fig. 3, system size $L = 60$, for different temperatures above T_f and current range $J < 0.03$, giving the estimate $\nu = 1.40(9)$. Inset: Finite-size scaling plot of the crossover current J_{nl} for different temperatures T and system sizes L, giving the estimate $\nu = 1.15(9)$. The dashed line is the fit used in the data collapse procedure.

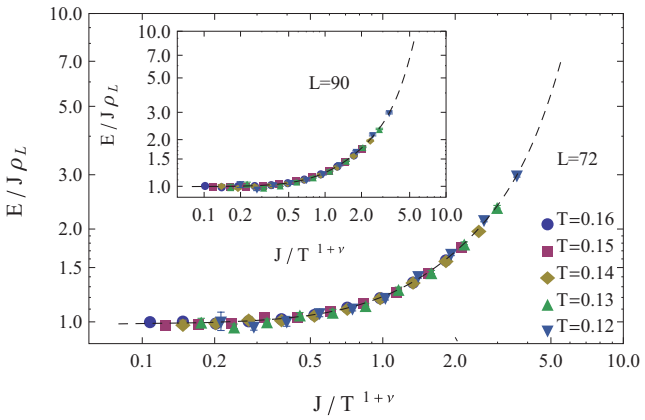

FIG. 7. (Color online) Scaling plot of the nonlinear resistivity E/J as in Fig. 6, for a larger system size $L = 72$, giving the estimate $\nu = 1.36(8)$. Inset: Same scaling plot for $L = 90$, giving the estimate $\nu = 1.33(8)$.

The scaling analysis of the whole nonlinear resistivity data is rather complicated in this case since the scaling function depends on two variables. To simplify the analysis,[27] we first estimate the temperature and finite-size behavior of the crossover current density J_{nl} where nonlinear behavior sets in, as the value of J where $E/J\rho_L = c$, a constant. Then, from Eq. (6) the finite-size behavior of J_{nl} can be expressed in the scaling form

$$J_{nl} L^{(1+\nu)/\nu} = \tilde{\tilde{g}}(L^{1/\nu} T). \tag{7}$$

The best data collapse according to the scaling in Eq. (7) provides an independent estimate of the critical exponent ν. The inset in Fig. 6 shows that indeed the values of J_{nl} for different system sizes and temperatures satisfy this scaling form with $\nu = 1.15(9)$. To check for systematic errors due to corrections to finite-size scaling, the data collapse was repeated dropping the smaller system sizes. Dropping system size $L = 24$ gives $\nu = 1.17(7)$ and $L = 24$ to $L = 36$ gives $\nu = 1.16(7)$. Since the resulting changes are small compared with the error bars, systematic errors of this kind are not significant for this range of system sizes. The two independent estimates of ν obtained above, 1.33(8) from the largest system size and 1.15(9) from finite-size scaling, are not compatible within the estimated errors. However, the former value could still be affected by finite-size effects. The latter value should be more accurate since it is based on finite-size scaling. This value is in reasonable agreement, within the estimated errors, with the critical exponent for the zero-temperature phase-coherence transition, $\nu_{ph} = 1.29(15)$, of the frustrated XY model obtained recently by correlation length calculations using equilibrium MC simulations.[19] The Arrhenius behavior for the linear resistivity ρ_L in Fig. 4 is also consistent with the exponential divergence of the relaxation time τ found in the equilibrium MC simulations.

Some experimental observations on ultrathin superconducting films with a triangular pattern of nanoholes[21] are consistent with the zero-temperature resistive transition for $f = 1/2$. In the regime where phase fluctuations of the superconducting order parameter are more important than amplitude fluctuations,[4,8] this system can be described by an array of superconducting "grains" coupled by Josephson junctions in a suitable geometry. The simplest model consists of a Josephson-junction array on a honeycomb lattice, with the triangular lattice of nanoholes corresponding to the lattice of pinning sites (plaquette centers in Fig. 1) and the number of flux quantum per unit cell of the nanohole lattice corresponding to the frustration parameter f of the array. In fact, the measured resistance of samples which are superconducting at low temperatures and low magnetic fields oscillates as a function of the magnetic field, displaying minima at integer values of f but no secondary minima at $f = 1/2$, as expected from the present results for the honeycomb JJ array. Moreover, for $f = 1/2$, the temperature dependence of the resistance shows the expected Arrhenius behavior, consistent with a vanishing critical temperature. However, the measured magnetoresistance does not display minima at $f = 1/3$, which would be expected from the above calculations for temperatures near $T_c(f = 1/3)$. Although the available temperatures in the experiments may not be sufficiently small to observe this feature, it could also be the effect of quenched disorder in the Josephson couplings. In fact, it was recently suggested that inhomogeneities in the film thickness could lead to significant variations in the weak links between superconducting islands.[21]

We have performed additional calculations to verify the qualitative effect of weak disorder of the Josephson couplings on the magnetoresistive behavior. We consider a simple random-coupling model, where J_{ij} in Eq. (1) is defined as $J_{ij} = J_o(1 \pm D)$, with equal probability, and disorder strength parameter D. The JJ array is still assumed to be on a perfect honeycomb lattice. The resistivity as a function of temperature was calculated by averaging over different realizations of the disorder. Figure 8 compares the temperature dependence of ρ_L obtained without current bias, from Eq. (3), for $f = 0, f = 1/3$, and $f = 1/2$, and different disorder strengths D. While the behavior characteristic of a finite-temperature transition for $f = 0$ and zero-temperature transition for $f = 1/2$ remains for increasing disorder, the resistive behavior for $f = 1/3$ changes to an Arrhenius form above a disorder strength $D \sim 0.35$. In this case, the magnetoresistance should only display minima at integer values of f, as observed experimentally,[21] which in turn suggests that coupling disorder should also play an important role in modeling other phase-coherence

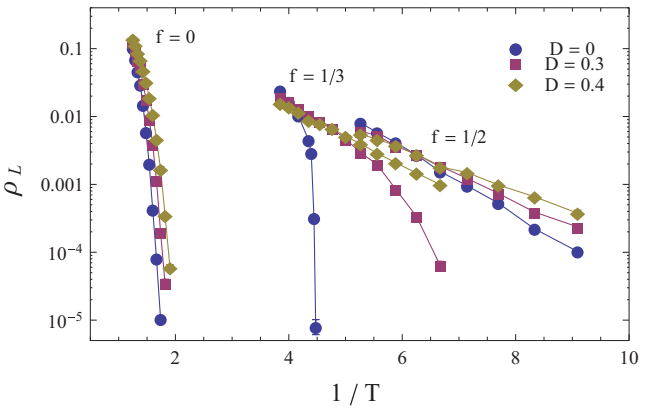

FIG. 8. (Color online) Temperature dependence of the linear resistivity ρ_L for different frustration parameters f and coupling disorder strengths D. System size $L = 60$.

properties of this system. When comparing the disorder strength D in the model with the thickness variations in the experimental system, geometrical disorder in the JJ array due to spatial irregularities of the system should also be taken into account. Weak positional disorder of the grains, for example, has significant effects both on phase-coherence and vortex order at nonzero values of frustration,[29–32] even when the Josephson coupling is uniform ($D = 0$). One then would expect that the combined effect of geometrical and Josephson-coupling disorder in the model will result in an Arrhenius behavior for $f = 1/3$ occurring at much lower values of D. These interesting effects and a more quantitative comparison of such a disorder model with the experimental system deserves further work.

IV. CONCLUSIONS

We have investigated the resistive behavior of Josephson-junction arrays on a honeycomb lattice using driven MC dynamics, focusing mainly on the $f = 1/2$ frustration and its relation to experiments on ultrathin superconducting films.[21] For $f = 1/3$, a resistive transition is found at nonzero temperature, as expected from early results of equilibrium MC simulations.[10] The estimated critical temperature is slightly below the melting transition of the commensurate vortex lattice,[19] suggesting two separated transitions. However, further work is required to obtain a more accurate estimate and to investigate the critical behavior in detail. For $f = 1/2$, the results are consistent with a transition scenario where the critical temperature vanishes and the linear resistivity shows thermally activated behavior. The thermal critical exponent ν of the zero-temperature transition estimated from a dynamical scaling analysis is in fair agreement with recent calculations from finite-size correlation length scaling.[19] A dynamical freezing at a lower temperature T_f was identified from deviations of the fluctuation-dissipation relation between linear resistivity and voltage autocorrelations. It should be pointed out that, since equilibrium data could not be obtained below T_f, a resistive transition at much lower temperatures cannot be ruled out. Moreover, since the scaling analysis assumes a second-order phase transition, a first-order resistive transition near or below T_f is also not excluded. The resistive behavior is qualitatively consistent with experimental observations in ultrathin superconducting films with a triangular lattice of nanoholes,[21] taking into account the effects of weak Josephson-coupling disorder. A more quantitative comparison to the experimental system, including geometrical disorder,[29–32] and the relation between the resistive behavior and the vortex structure[18] for $f = 1/2$, as well as $f = 1/3$, require further work.

ACKNOWLEDGMENTS

This work was supported by Fundação de Amparo à Pesquisa do Estado de São Paulo (FAPESP, Grant No. 07/08492-9) and computer facilities from Centro Nacional de Processamento de Alto Desempenho em São Paulo (CENAPAD-SP).

[1] H. S. J. Zant, H. A. Rijken, and J. E. Mooij, J. Low Temp. Phys. **82**, 67 (1991).
[2] M. Tinkham, D. W. Abraham, and C. J. Lobb, Phys. Rev. B **28**, 6578 (1983).
[3] I. C. Baek, Y. J. Yun, and M. Y. Choi, Phys. Rev. B **69**, 172501 (2004).
[4] M. Giroud, O. Buisson, Y. Y. Wang, and B. Pannetier, J. Low Temp. Phys. **87**, 683 (1992).
[5] F. Yu, N. E. Israeloff, A. M. Goldman, and R. Bojko, Phys. Rev. Lett. **68**, 2535 (1992).
[6] X. S. Ling, H. J. Lezec, M. J. Higgins, J. S. Tsai, J. Fujita, H. Numata, Y. Nakamura, Y. Ochiai, C. Tang, P. M. Chaikin, and S. Bhattacharya, Phys. Rev. Lett. **76**, 2989 (1996).
[7] Y. Xiao, D. A. Huse, P. M. Chaikin, M. J. Higgins, S. Bhattacharya, and D. Spencer, Phys. Rev. B **65**, 214503 (2002).
[8] V. J. Emery and S. A. Kivelson, Nature (London) **374**, 434 (1995).
[9] S. Teitel and C. Jayaprakash, Phys. Rev. Lett. **51**, 1999 (1983); Phys. Rev. B **27**, 598 (1983).
[10] W. Y. Shih and D. Stroud, Phys. Rev. B **32**, 158 (1985); **30**, 6774 (1984).
[11] V. I. Marconi and Daniel Domínguez, Phys. Rev. Lett. **87**, 017004 (2001); G. S. Jeon, J. S. Lim, H. J. Kim, and M. Y. Choi, Phys. Rev. B **66**, 024511 (2002); M. B. Luo and Q. H. Chen, Eur. Phys. J. B **35**, 201 (2003).
[12] T. C. Halsey, Phys. Rev. Lett. **55**, 1018 (1985).
[13] P. Gupta, S. Teitel, and M. J. P. Gingras, Phys. Rev. Lett. **80**, 105 (1998).
[14] S. Y. Park, M. Y. Choi, B. J. Kim, G. S. Jeon, and J. S. Chung, Phys. Rev. Lett. **85**, 3484 (2000).
[15] E. Granato, Phys. Rev. B **75**, 184527 (2007); **54**, R9655 (1996).
[16] E. Granato, Phys. Rev. Lett. **101**, 027004 (2008).
[17] R. W. Reid, S. K. Bose, and B. Mitrović, J. Phys.: Condens. Matter **9**, 7141 (1997).
[18] S. E. Korshunov and B. Douçot, Phys. Rev. Lett. **93**, 097003 (2004); S. E. Korshunov, Phys. Rev. B **85**, 134526 (2012).
[19] E. Granato, Phys. Rev. B **85**, 054508 (2012).
[20] T. I. Baturina, D. W. Horsell, D. R. Islamov, I. V. Drebushchak, Yu. A. Tsaplin, A. A. Babenko, Z. D. Kvon, A. K. Savchenko, and A. E. Plotnikov, Physica B **329**, 1496 (2003); T. I. Baturina, V. M. Vinokur, A. Yu. Mironov, N. M. Chtchelkatchev, D. A. Nasimov, and A. V. Latyshev, Europhys. Lett. **93**, 47002 (2011).
[21] M. D. Stewart, Jr., Z. Long, J. M. Valles, Jr., A. Yin, and J. M. Xu, Phys. Rev. B **73**, 092509 (2006); H. Q. Nguyen, S. M. Hollen, M. D. Stewart, Jr., J. Shainline, A. Yin, J. M. Xu, and J. M. Valles, Jr., Phys. Rev. Lett. **103**, 157001 (2009); S. M. Hollen, H. Q. Nguyen, E. Rudisalle, M. D. Stewart, Jr., J. Shainline, J. M. Xu, and J. M. Valles, Jr., Phys. Rev. B **84**, 064528 (2011).
[22] J. R. Lee and S. Teitel, Phys. Rev. Lett. **66**, 2100 (1991).
[23] E. Granato, Phys. Rev. B **69**, 144203 (2004).
[24] W. M. Saslow, M. Gabay, and W.-M. Zhang, Phys. Rev. Lett. **68**, 3627 (1992).
[25] E. Granato, Phys. Rev. B **58**, 11161 (1998).

[26]R. A. Hyman, M. Wallin, M. P. A. Fisher, S. M. Girvin, and A. P. Young, Phys. Rev. B **51**, 15304 (1995); D. S. Fisher, M. P. A. Fisher, and D. A. Huse, *ibid.* **43**, 130 (1991).
[27]C. Wengel and A. P. Young, Phys. Rev. B **56**, 5918 (1997).
[28]M. P. Nightingale and H. W. J. Blöte, Phys. Rev. B **54**, 1001 (1996).
[29]E. Granato and J. M. Kosterlitz, Phys. Rev. B **33**, 6533 (1986); Phys. Rev. Lett. **62**, 823 (1989).
[30]M. G. Forrester, H. J. Lee, M. Tinkham, and C. J. Lobb, Phys. Rev. B **37**, 5966 (1988); S. P. Benz, M. G. Forrester, M. Tinkham, and C. J. Lobb, *ibid.* **38**, 2869 (1988).
[31]S. E. Korshunov and T. Nattermann, Phys. Rev. B **53**, 2746 (1996).
[32]P. Gupta and S. Teitel, Phys. Rev. Lett. **82**, 5313 (1999).